

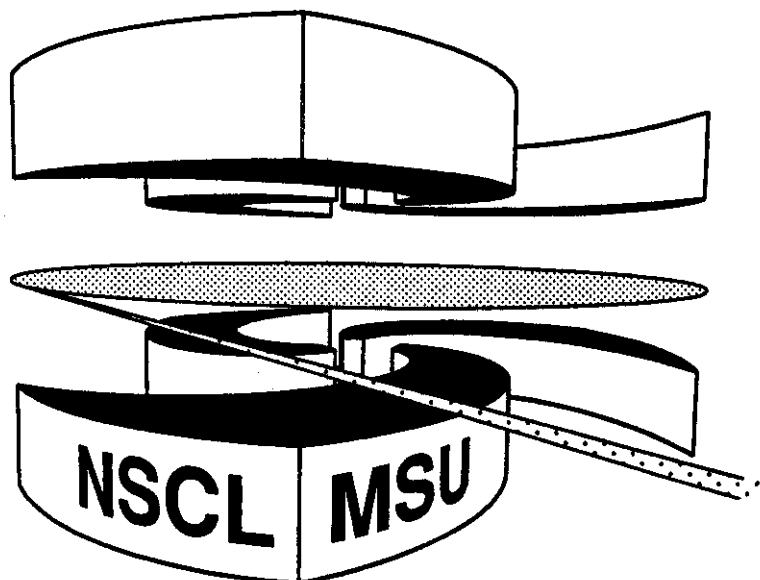


# Michigan State University

National Superconducting Cyclotron Laboratory

## ELECTROMAGNETIC EXCITATION OF $^{11}\text{Li}$

**A. GALONSKY, D. SACKETT, K. IEKI, C.A. BERTULANI,  
H. ESBENSEN, J.J. KRUSE, W.G. LYNCH,  
D.J. MORRISSEY, N.A. ORR, B.M. SHERRILL,  
H. SCHULZ, A. SUSTICH, J.A. WINGER, Á. HORVÁTH,  
F. DEÁK, Á KISS, Z. SERES, J.J. KOLATA,  
R.E. WARNER, and D.L. HUMPHREY**



## ELECTROMAGNETIC EXCITATION OF $^{11}\text{Li}^*$

A. GALONSKY, D. SACKETT, K. IEKI, C. A. BERTULANI, H. ESBENSEN, J. J. KRUSE, W.G. LYNCH, D. J. MORRISSEY, N.A. ORR, B.M. SHERRILL, H. SCHULZ, A. SUSTICH and J. A. WINGER

*National Superconducting Cyclotron Laboratory  
and Department of Physics and Astronomy  
Michigan State University, East Lansing, MI 48824-1321, USA*

A. HORVÁTH, F. DEÁK, Á. KISS

*Eötvös University  
Puskín utca 5-7, H-1088  
Budapest 8, Hungary*

Z. SERES

*KFKI Research Institute for Particle and Nuclear Physics  
of the Hungarian Academy of Sciences  
H-1525 Budapest 114, Hungary*

J. J. KOLATA

*University of Notre Dame  
Notre Dame, IN 46556, USA*

R. E. WARNER

*Department of Physics  
Oberlin College  
Oberlin, OH 44074, USA*

D. L. HUMPHREY

*W. Kentucky University  
Bowling Green, KY 42101, USA*

### ABSTRACT

In a Coulomb dissociation of  $^{11}\text{Li}$  the complete kinematics were measured. From the electric dipole excitation spectrum and from an observed systematic excess of  $^9\text{Li}$  velocity above neutron velocity, it is concluded the proposed soft dipole mode is not present. The  $^9\text{Li}$  and neutron momentum distributions in the  $^{11}\text{Li}$  rest frame are fitted by a phase space model rather than a dineutron model.

\*Main content of invited talk given by A. Galonsky at the Third International Conference on Radioactive Beams held at Michigan State University, May 24-27, 1993.

## 1. Introduction

Figure 1 shows the experimental areas in which the RNB experiments have been done at MSU. The experiments which had been performed up to January, 1993 are indicated. With the A1200 being the feeder of all cyclotron beams to all parts of the laboratory, RNB experiments have by now been performed in all the experimental vaults. I will describe one performed in the N4 Vault, the vault partially visible in the northeast corner of Fig. 1. This is an experiment on the electromagnetic excitation of  $^{11}\text{Li}$ <sup>1,2</sup>

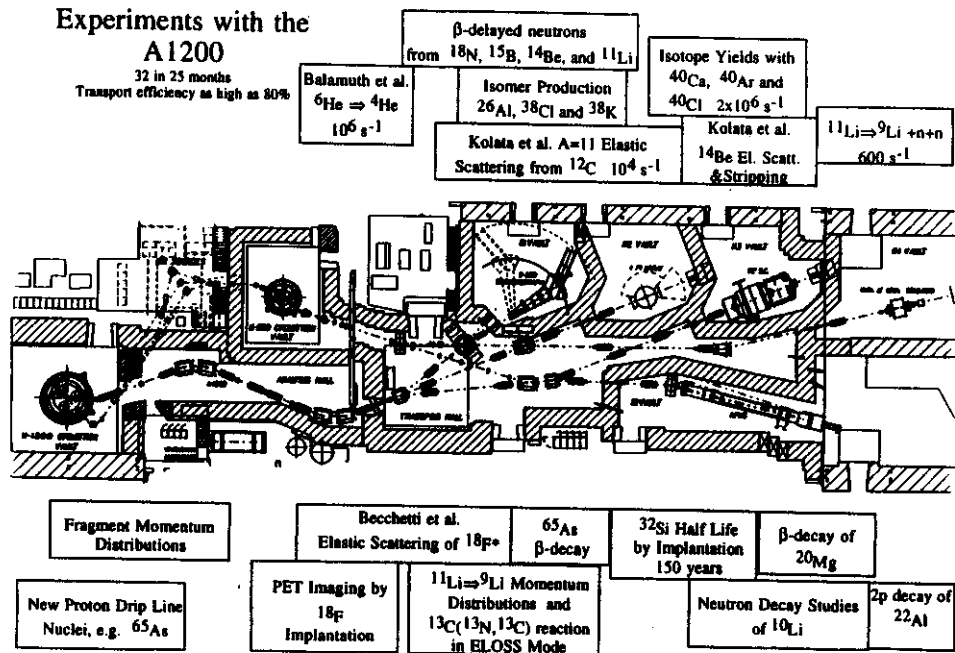


Fig. 1: Layout of the NSCL experimental area with locations of RNB experiments (up to January, 1993) indicated.

There were two motivations for the experiment. One was to measure the parameters of the proposed soft dipole resonance<sup>3,4,5</sup>, such as its resonance energy and width. The other was to find evidence for, or against, a bound dineutron<sup>3</sup>.

In the giant dipole resonance the photon drives all the protons against all the neutrons in a nucleus. From the systematics on restoring force and inertia, the resonant energy in  $^{11}\text{Li}$  would be expected to be  $\sim 25$  MeV. The soft dipole resonance is another collective resonance in which the restoring force on the oscillating protons is provided by the two halo neutrons. This restoring force is so weak that the resonant energy may be only  $\sim 1$  MeV. Schematics of these two electric dipole resonances are shown in Fig. 2. The latter resonance should occur only when the valence neutrons are so lightly bound that they form a halo around the charged core.

The structure of the giant dipole resonance has been studied for more than four decades by measurement of the excitation function for photon absorption. The spectrum in the top part of Fig. 3 was published in 1962<sup>6</sup>. Photoneutron cross section

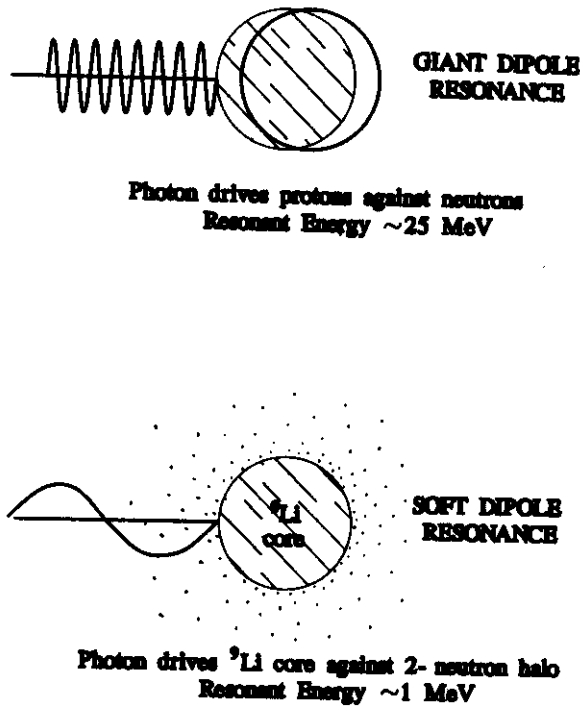


Fig. 2: The mechanics of the giant dipole resonance and the proposed soft dipole resonance.

is plotted against photon energy. Thresholds for emission of 1, 2, and 3 neutrons are indicated. In the bottom part of the figure are sketches of the energetics for photon-neutron absorption in <sup>197</sup>Au and in <sup>11</sup>Li. Although the two sketches represent the same process, a <sup>11</sup>Li target is not available. Instead, we reverse the process, using <sup>11</sup>Li as the beam and obtain virtual photons from a high-Z target nucleus; Pb in this case.<sup>7</sup> The dipole strength function is obtained from the equation

$$\text{Photon Absorption } \sigma = (\text{E1 Strength Function}) * (\text{Virtual Photon Spectrum.})$$

Although the photon spectrum is calculable<sup>8</sup>, we have no control over the energy of the photon absorbed in a given event.  $E_\gamma$  is discovered only after analysis of the event; we use the relation (see bottom, right of Fig. 3)

$$E_\gamma = E_{decay} + S_{2n}.$$

A histogram of  $E_\gamma$  values gives us the photon absorption  $\sigma$ . Although  $S_{2n}$  is known to be about 1/3 MeV<sup>9</sup>, a determination of  $E_{decay}$  requires the complete kinematics of the decay into <sup>9</sup>Li and two neutrons to be measured for each event.

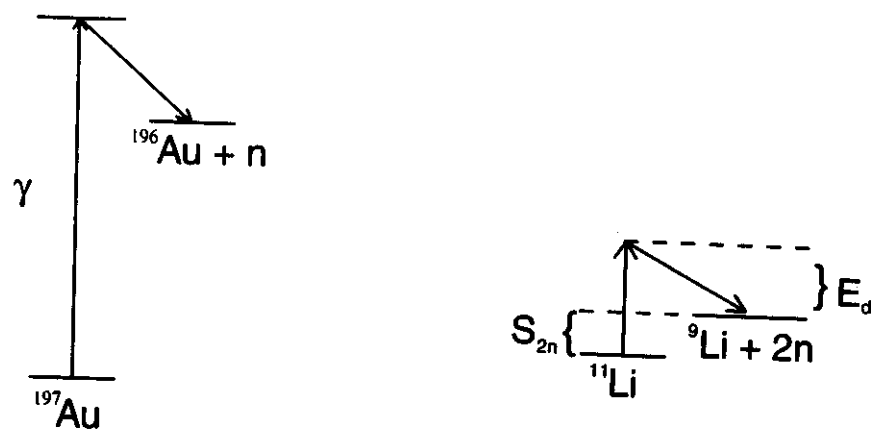
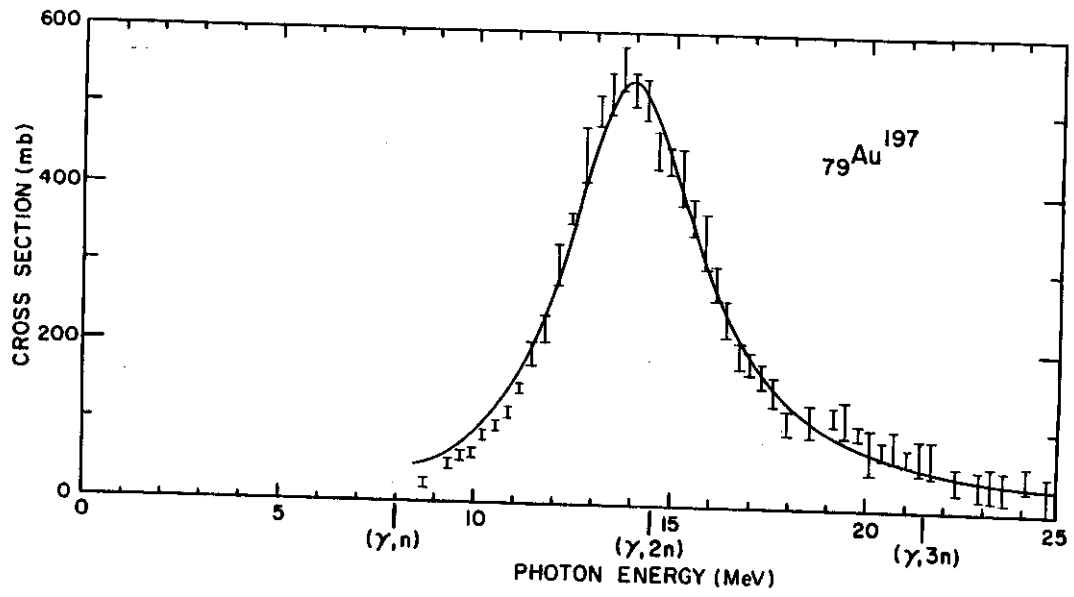


Fig. 3: Giant-dipole data from Ref.6 and schematics of the photoneutron process in  $^{197}\text{Au}$  and in  $^{11}\text{Li}$ .

## 2. The Experiment

The complete kinematics were measured with the apparatus illustrated in Fig. 4. The beam was incident from the lower right at an energy of 30 MeV/nucleon. Each  $^{11}\text{Li}$  projectile had already generated a time-of-flight start signal in a scintillator. From its signal in the  $\Delta E$  Si detector, we could determine its kinetic energy, and from the two PPAC(x,y) signals its direction. Energy and direction of the  $^9\text{Li}$  decay fragment were measured with the Si/CsI telescope; the Si had 16x and 16y strips, effectively defining 256 pixels of angular width  $1.2^\circ$ . Energy and direction of each neutron were determined from flight time and neutron detector (liquid scintillator) position.

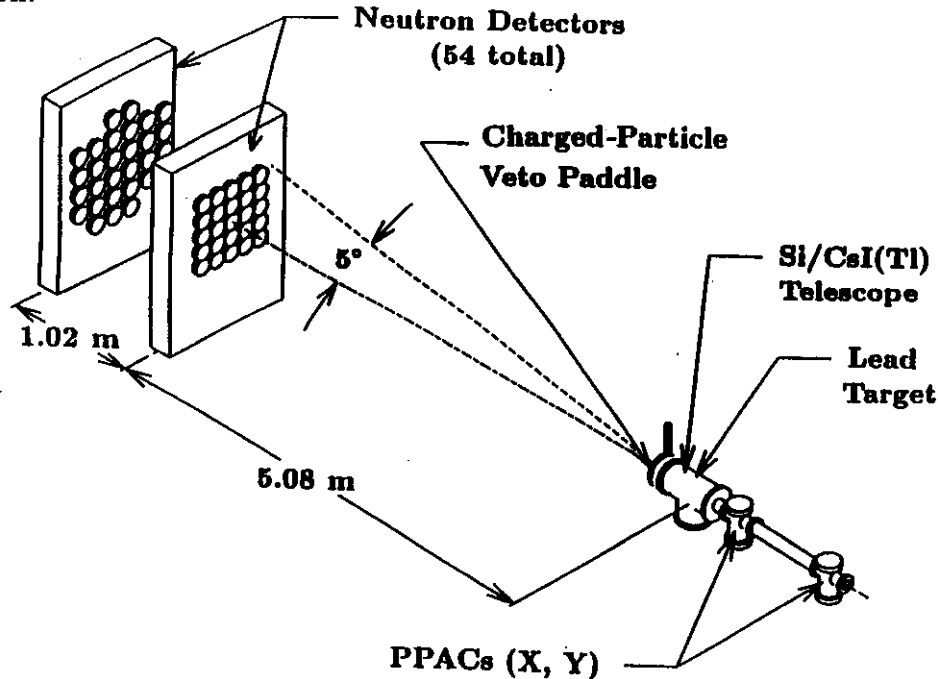


Fig. 4: Detector setup. The  $^{11}\text{Li}$  beam enters from the lower right.

Decay-energy spectra are shown in Fig. 5. An individual event of breakup into  $^9\text{Li} + n + n$  in the fragment telescope is indistinguishable from one in the Pb target. Therefore, we had to collect events with target ((a) in Fig. 5) and without target (b) and take the difference(c). (c) has a net of about 2,000 events.

## 3. Results

### 3.1. E1 Strength Function

The spectrum is repeated, with a log scale and with different binning, in the top half of Fig. 6. In the bottom half are three possible elastic dipole strength functions. The dashed line represents a direct breakup model<sup>10</sup>, the dotted one a correlated-state model<sup>11</sup>, and the solid curve depicts an empirical resonance. To compare a

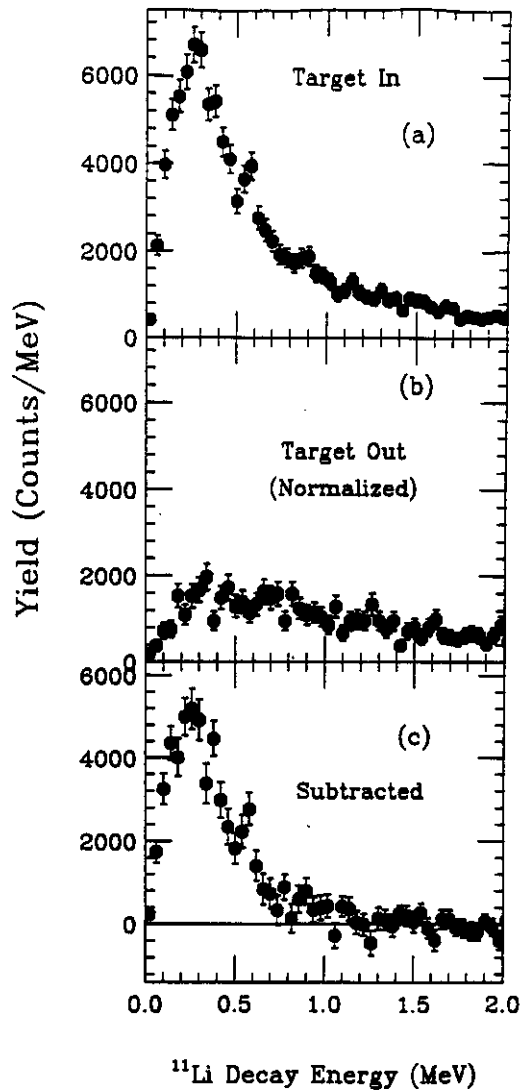


Fig. 5: Decay energy spectra.

dipole strength function with our data, we must multiply the strength function by the virtual photon spectrum and by our detector response function. Because the angular acceptance of the neutron array is only  $5^\circ$ , the response is a rapidly decreasing function of decay energy. A neutron emitted with 0.3 MeV and at  $90^\circ$  in the  $^{11}\text{Li}$  rest frame, for example, will have an angle of  $\sqrt{0.3/30} = 0.1$  or  $6^\circ$  in the laboratory—it will miss the neutron array. When the solid curve in the bottom half of Fig. 6 was Monte-Carloed through our detector response function (and the photon spectrum), it produced the solid curve that fits our data so well in the top half. The solid curve in the bottom half is the dipole strength function determined by our data. A theoretical model that produces a dipole strength function in agreement with this curve is in agreement with our data.

To obtain the fit that is shown we assumed a Breit-Wigner resonance shape and searched on its two parameters—resonance energy and width. The results were  $E_d=0.7$  MeV ( $E_x=E_d+S_{2n} \cong 1.0$  MeV) and  $\Gamma=0.8$  MeV. It is instructive to compute the times

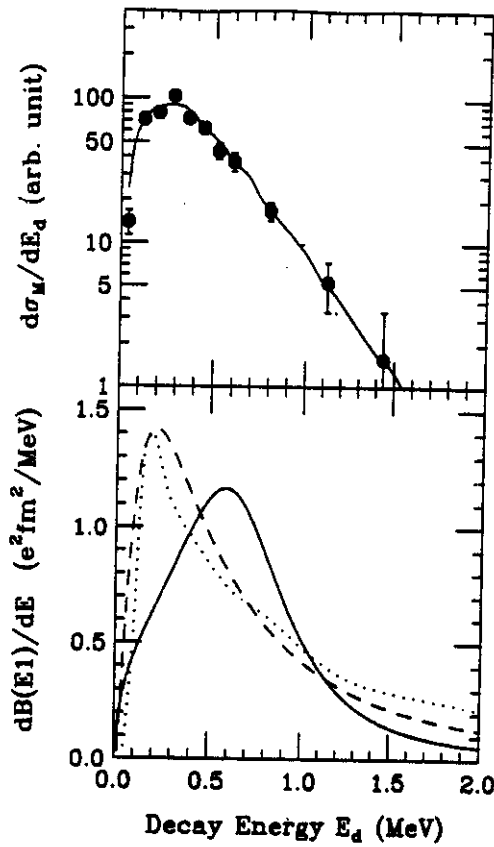


Fig. 6: Decay energy spectrum above and electric dipole strength function below. The solid curve below results from a Breit-Wigner resonance function with  $E_{res}=0.7$  MeV and  $\Gamma=0.8$  MeV. This curve, with the virtual photon spectrum and the detector response function, produced the data-fitting curve above.

corresponding to these energies. If our resonance represents the soft dipole resonance, the period of oscillation of the  ${}^9\text{Li}$  core in the two-neutron halo may be obtained as follows:

$$E_x = \hbar\omega = \hbar 2\pi/T; T=2\pi\hbar c/E_x c \cong 1200 \text{ fm}/c$$

From the width of the state we got its lifetime:

$$\Gamma\tau = \hbar; \tau = \frac{\hbar c}{\Gamma c} = \frac{200}{0.8} = 250 \text{ fm}/c$$

Therefore, the state lives for only 1/5 of an oscillation, on average. Such a short lifetime does not support the picture of a core oscillating back and forth in the halo.

### 3.2. Post-Breakup Coulomb Acceleration

An observation that was not expected in the experiment is shown in the top half of Fig. 7. The  ${}^9\text{Li}$  velocity is systematically higher than the average neutron velocity. To check for a possible instrumental bias we ran a computer simulation of un-accelerated events and got the histogram in the figure. It is symmetrical and



centered on zero. Of course, our fragment and neutron velocities were measured by different means, the fragment by the energy deposited in a calibrated CsI scintillator, the neutron by its flight time. Although our estimates of the systematic error in each of the two measurements could not account for the observed velocity difference, we were able to construct an experimental check, as illustrated in the bottom half of Fig. 7. There we compare the initial center-of-mass velocity, ( $^{11}\text{Li}$  velocity), with the final CM velocity. Since the latter value depends mostly on the  $^9\text{Li}$  velocity, which comes from energy deposition, and the former (and the neutron velocity) comes from time-of-flight measurement, the almost perfect centering of this distribution is reassuring. The width of the distribution is a measure of our instrumental velocity difference resolution.

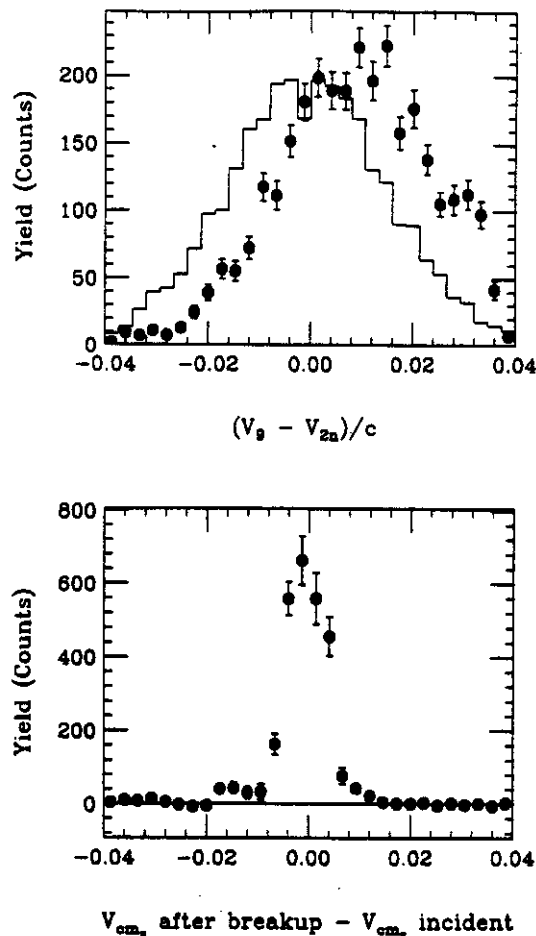


Fig. 7: (a) the spectrum for the velocity difference  $V_9 = V_{2n}$ , where  $V_{2n}$  is the average velocity of the two detected neutrons. The histogram is the result of a simulation using an initial distribution with the velocity difference peaked at zero. (b) The spectrum for the z-component of the center of mass velocity before breakup subtracted from the center of mass velocity after breakup.

We have no choice but to take the observed velocity difference seriously and try

to interpret it. One possible interpretation is illustrated by the simplified sketch in Fig. 8. This shows that if the lifetime of the excited  $^{11}\text{Li}$  is short enough, break-up will occur while the Li is still high on the Coulomb Hill.  $^9\text{Li}$  will receive a Coulomb acceleration, and the neutrons will not. We can work this idea backwards from the measured value of  $v_9 - v_{2n}$ . That value determines the Coulomb energy, which determines  $r$  in Fig. 8, and  $r$  determines  $\tau$ , the result being  $\tau \sim 50 \text{ fm}/c$ . From the width of the "resonance" we deduced a  $\tau$  of  $250 \text{ fm}/c$ . More doubt is cast on the existence of a resonant state. The peaks in Figs. 5 and 6 look like a resonance, but an excitation function must rise from zero at threshold and, because of a sum rule, eventually come down again. The Coulomb acceleration method of lifetime determination is independent of whether or not there is a soft-dipole resonance, and, of course,  $50 \text{ fm}/c$  is only 4% of the  $1200 \text{ fm}/c$  oscillation period for a soft-dipole resonance at  $E_x = 1 \text{ MeV}$ . We conclude that we have observed a direct break-up of  $^{11}\text{Li}$ , rather than a soft-dipole resonance.

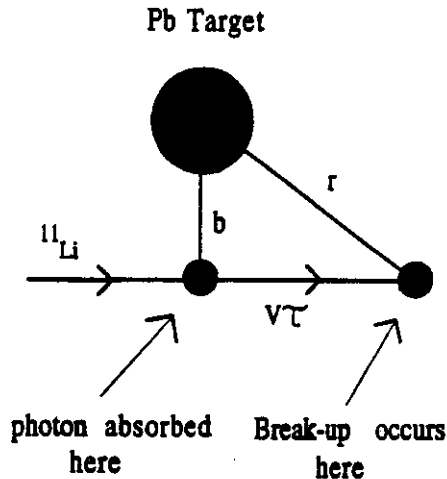


Fig. 8: A schematic view of a  $^{11}\text{Li}$  breakup. The average impact parameter is  $b=20 \text{ fm}$ . The distance from the Pb nucleus to the breakup point is denoted by  $r$ .  $V$  is the beam velocity and  $\tau$  is the meanlife of the excited  $^{11}\text{Li}$ .

### 3.3. Momentum Distributions

From the decay kinematics we determined the momentum distributions of  $^9\text{Li}$  and of a neutron in the  $^{11}\text{Li}$  rest frame. These are shown in Fig. 9 (the points) and compared with two models. The solid histograms are the predictions of the standard three-body phase-space model, as in  $\beta$  decay. For the dashed histograms a two-body decay, in which  $^9\text{Li}$  recoiled against a dineutron, was assumed. We see that the phase-space model fits the data and the dineutron model does not. Therefore our data display no evidence for a dineutron in the structure of  $^{11}\text{Li}$ .

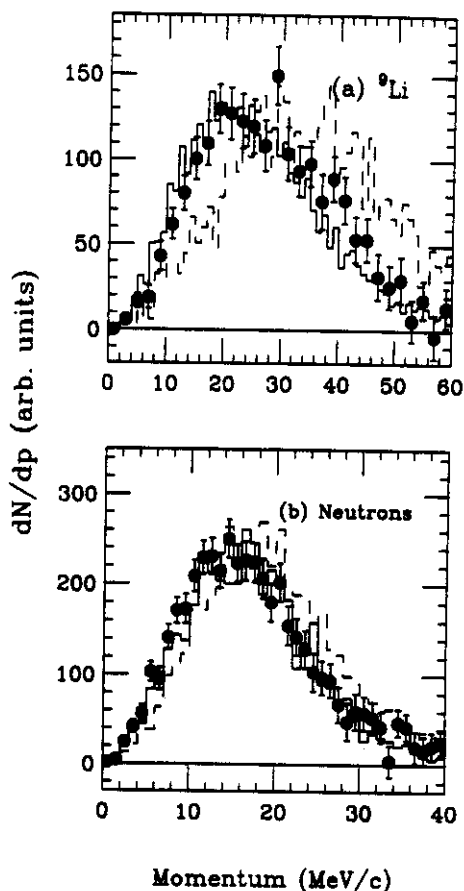


Fig. 9:  ${}^9\text{Li}$  (part a) and neutron (part b) momentum distributions in the  ${}^{11}\text{Li}$  rest frame. The histograms result from Monte Carlo simulations of  ${}^{11}\text{Li}$  breakup with the decay energy partitioned according to (solid histograms) a 3-body phase space distribution and (dashed histograms) a 2-body  ${}^9\text{Li}$ -dineutron “distribution.”

#### 4. Summary

From a measurement of the 3-body decay kinematics of photo-excited  ${}^{11}\text{Li}$  into  ${}^9\text{Li} + n + n$  we determined the  $E1$  Strength function up to about one MeV above threshold. We also measured the relative velocity spectrum between  ${}^9\text{Li}$  and halo neutrons and found a net excess of  ${}^9\text{Li}$  velocity over  $n$  velocity. From these two observations we conclude that there is no soft-dipole resonance in  ${}^{11}\text{Li}$ .

We determined  ${}^9\text{Li}$  and neutron momentum distributions in the  ${}^{11}\text{Li}$  rest frame and found that a  ${}^9\text{Li}$ -dineutron model of  ${}^{11}\text{Li}$  does not fit these distributions.

\*The material in this paper was presented in a poster session and as the main subject of an invited talk by A. Galonsky.

## 5. References

- [1] K. Ieki, D. Sackett, A. Galonsky, C. A. Bertulani, J. J. Kruse, W. G. Lynch, D. J. Morrissey, N. A. Orr, H. Schultz, B. M. Sherrill, A. Sustich, J. A. Winger, F. Deák, Á. Horváth, Á. Kiss, Z. Seres, J. J. Kolata, R. E. Warner and D. L. Humphrey, *Phys. Rev. Lett.* 70,730(1993).
- [2] D. Sackett, K. Ieki, A. Galonsky, C. A. Bertulani, H. Esbensen, J. J. Kruse, W. G. Lynch, D. J. Morrissey, N. A. Orr, B. M. Sherrill, H. Schulz, A. Sustich, J. A. Winger, F. Deák, Á. Horváth, Á. Kiss, Z. Seres, J. J. Kolata, R. E. Warner, D. L. Humphrey; *Phys. Rev. C*, July, 1993.
- [3] P. G. Hansen and B. Jonson, *Europhys. Lett.* 4, 409 (1987).
- [4] T. Kobayashi, S. Shimoura, I. Tanihata, K. Katori, K. Matsuta, T. Minamisono, K. Sugimoto, W. Muller, D. L. Olson, T. J. M. Symons and H. Wieman, *Phys. Lett.* B232, 51 (1989).
- [5] K. Ikeda, *Nucl. Phys.* A538, 355c (1992).
- [6] S. C. Fultz, R. L. Bramblett, J. T. Caldwell and N. A. Kerr, *Phys. Rev.* 127, 1273 (1962).
- [7] G. Baur, C. A. Bertulani and H. Rebel, *Nucl. Phys.* A458, 188 (1986).
- [8] C. A. Bertulani and G. Baur, *Phys. Rep.* 163, 299 (1988).
- [9] T. Kobayashi, *Nucl. Phys.* A538, 343c (1992). K. Matsuta, T. Minamisono, K. Sugimoto, W. Muller, D.L. Olson, T. J. M. Symons and H. Wieman, *Phys. Lett.* B232, 51 (1989).
- [10] C. A. Bertulani, G. Baur and M. S. Hussein, *Nucl. Phys.* A526, 751 (1991).
- [11] H. Esbensen and G. F. Bertsch, *Nucl. Phys.* A542, 310 (1992).